LAWRENCE
LIVERMORE
NATIONAL
LABORATORY

UCRL-PROC-225429

Corrosion Resistances of Iron-Based Amorphous Metals with Yttrium and Tungsten Additions in Hot Calcium Chloride Brine & Natural Seawater: Fe48Mo14Cr15Y2C15B6 and W-Containing Variants

J. C. Farmer, J. Haslam, S. Day, T. Lian, C. Saw, P. Hailey, J-S. Choi, N. Yang, C. Blue, W. Peter, J. Payer, D. J. Branagan

October 20, 2006

210th Meeting of The Electrochemical Society, 2006 Joint International Meeting
Cancun, Mexico
October 29, 2006 through November 3, 2006

Corrosion Resistances of Iron-Based Amorphous Metals with Yttrium and Tungsten Additions in Hot Calcium Chloride Brine & Natural Seawater: $Fe_{48}Mo_{14}Cr_{15}Y_2C_{15}B_6$ and W-Containing Variants

J. Farmer, J. Haslam, S. Day, T. Lian, C. Saw, P. Hailey and J-S. Choi
Lawrence Livermore National Laboratory, Livermore, CA, 94550

N. Yang
Sandia National Laboratory, Livermore, CA, 94550

C. Blue and W. Peter
Oak Ridge National Laboratory, Oak Ridge, TN, 37830

J. Payer
Case Western Reserve University, Cleveland, OH, 44106

D. Branagan
The NanoSteel Company, Idaho Falls, ID, 83402

Abstract

Yttrium-containing SAM1651 ($Fe_{48.0}Cr_{15.0}Mo_{14.0}B_{6.0}C_{15.0}Y_{2.0}$), has a critical cooling rate (CCR) of approximately 80 Kelvin per second, while SAM2X5 ($Fe_{49.7}Cr_{17.7}Mn_{1.9}Mo_{7.4}W_{1.6}B_{15.2}C_{3.8}Si_{2.4}$) with no yttrium has a higher critical cooling rate of approximately 600 Kelvin per second. SAM1651's low CCR enables it to be rendered as a completely amorphous material in practical materials processes. Chromium (Cr), molybdenum (Mo) and tungsten (W) provide corrosion resistance; boron (B) enables glass formation; and rare earths such as yttrium (Y) lower critical cooling rate (CCR). The passive film stability of these Fe-based amorphous metal formulations have been found to be superior to that of conventional stainless steels, and comparable to that of Ni-based alloys, based on electrochemical measurements of the passive film breakdown potential and general corrosion rates.

Introduction

The outstanding corrosion possible with amorphous metals has been recognized for many years [1-3]. A number of other iron-based amorphous metals have been published, including several with very good corrosion resistance. Examples include: thermally sprayed coatings of Fe-10Cr-10-Mo-(C,B) which were explored as early as 1996 by Kishitake et al. [4]; bulk Fe-Cr-Mo-C-B [5]; and Fe-Cr-Mo-C-B-P [6]. These authors have corroborated the outstanding corrosion resistance of the amorphous Fe-Cr-Mo-C-B-P alloys [5]. Nickel-based amorphous metals have also been developed which exhibit exceptional corrosion performance in acids [7].

Several Fe-based amorphous metal formulations have been found that appear to have very good corrosion resistance, based on measurements of the passive film breakdown potential, the corrosion rate and performance during salt fog testing [8-10]. These

formulations use chromium (Cr), molybdenum (Mo), and tungsten (W) to provide corrosion resistance, boron (B) to enable glass formation, and yttrium to lower the critical cooling rate (CRR). SAM1651 ($Fe_{48.0}Cr_{15.0}Mo_{14.0}B_{6.0}C_{15.0}Y_{2.0}$), has very low critical cooling rate of approximately 80 Kelvin per second, due to the addition of yttrium. The SAM1651 formulation has a similar elemental composition as the Y-containing Fe-based amorphous metal formulation discussed in the literature [11-13]. These rare-earth containing materials have been selected with particular emphasis on glass forming ability, thermal stability, hardness, and corrosion resistance, all under conditions of interest.

Experimental

Procedures

Melt Spinning Process. Maximum cooling rates of one million Kelvin per second (10^6 K/s) have been achieved with melt spinning, and is therefore ideal for producing amorphous metals over a very broad range of compositions. This process has been used as methods to synthesize completely amorphous, Fe-based, corrosion-resistant alloys with near theoretical density, thereby enabling the effects of coating morphology on corrosion resistance to be separated from the effects of elemental composition. The melt-spun ribbon (MSR) samples produced with this equipment are several meters long, several millimeters wide and approximately 150 microns thick. In contrast, the cooling rate in a typical thermal spray process such as HVOF are on the order of ten thousand Kelvin per second (10^4 K/s). The compositional range of materials that can be rendered as amorphous metals with thermal spray is therefore more restricted.

Thermal Spray Process. The coatings discussed here were made with the high-velocity oxy-fuel (HVOF) process, which involves a combustion flame, and is characterized by gas and particle velocities that are three to four times the speed of sound (mach 3 to 4). This process is ideal for depositing metal and cermet coatings, which have typical bond strengths of 5,000 to 10,000 pounds per square inch (5-10 ksi), porosities of less than one percent (< 1%) and extreme hardness.

Energy Dispersive Spectroscopy. Semi-quantitative elemental composition was determined with Energy Dispersive Spectroscopy (EDS). Microanalysis of each sample was performed at three randomly-selected locations at 10,000X magnification. Compositional analysis was performed on the smoother side of each melt-spun ribbon (MSR), as the rougher sides were found in some cases to be contaminated with small amounts of copper, presumably from contact with the copper wheel during the melt spinning process. Values of light elements such as boron and carbon were assumed and used to calculate the compositional values for the remaining heavier elements, with the relative ratios of the heavier elements reliably established with EDS.

X-Ray Diffraction. The basic theory for X-ray diffraction (XRD) of amorphous materials is well developed and has been published in the literature [16-17]. In an amorphous material, there are broad diffraction peaks. Diffraction was done with CuK_α X-rays, a graphite analyzing crystal, and a Philips vertical goniometer, using the Bragg-Bretano method. The X-ray optics were self-focusing, and the distance between the X-ray focal point to the sample position was equal to the distance between the sample position and the receiving slit for the reflection mode. Thus, the intensity and resolution was

optimized. Parallel vertical slits were added to improve the scattering signal. Step scan is performed from 20 to 90° (2θ) with step size of 0.02° at 4 to 10 seconds per point, depending on the amount of sample. The samples are loaded onto low quartz holders. This is because the expected intensity is very low and hence background scattering needs to be minimized.

Thermal Analysis. The thermal properties of these Fe-based amorphous metals have been determined. Thermal analysis of these Fe-based amorphous metals, with differential scanning calorimetry (DSC) or differential thermal analysis (DTA), allows determination of important thermal properties such as the glass transition temperature (T_g), crystallization temperature (T_x), and the melting point (T_m). Results from the thermal analysis of amorphous samples provides initial assessment of the glass forming ability of these materials through conventional metrics, such as the reduced glass transition temperature ($T_{rg} = T_g/T_L$).

Mechanical Properties. Hardness is an important parameter that has impact on wear resistance, as well as the resistance to erosion-corrosion. Vickers micro-hardness (HV) is the standard approach used to assess the hardness of thermal spray coatings. In the case of thermal spray coatings, a 300-gram load is frequently used, since it is believed that this load and the affected area are large enough to produce a measurement that is averaged over any macro-porosity that may be present. Micro-hardness measurements with a 100-gram load are also valuable, since it is believed that this load and the affected area are smaller, and therefore capable of sampling bulk material properties.

Cyclic Polarization. Cyclic polarization (CP) measurements have been based on a procedure similar to ASTM (American Society for Testing and Materials) G 5 standard with slight modification [18-19]. The ASTM G 5 standard calls for a 1 N H_2SO_4 electrolyte, whereas synthetic bicarbonate, sulfate-chloride, chloride-nitrate, and chloride-nitrate solutions, with sodium, potassium and calcium cations, as well as natural seawater have been used for this investigation. The natural seawater used in these tests was obtained directly from Half Moon Bay along the northern coast of California. Furthermore, the ASTM G 5 standard calls for the use of de-aerated solutions, whereas aerated and de-aerated solutions were used here. All data has been interpreted in a manner consistent with the published literature [20-21].

Temperature-controlled borosilicate glass (Pyrex) electrochemical cells were used for cyclic polarization and other similar electrochemical measurements. This cell has three electrodes, a working electrode (test specimen), the reference electrode, and the counter electrode. A standard silver silver-chloride electrode, filled with near-saturation potassium chloride solution, is used as the reference, and communicates with the test solution via a Luggin probe placed in close proximity to the working electrode, thereby minimizing Ohmic losses. The electrochemical cell is equipped with a water-cooled junction to maintain reference electrode at ambient temperature, thereby maintaining integrity of the potential measurement, and a water-cooled condenser to prevent the loss of volatile species from the electrolyte.

To assess the sensitivity of these iron-based amorphous metals to devitrification, which can occur at elevated temperature, melt-spun ribbons of Fe-based amorphous metals were intentionally devitrified by heat treating them at various temperatures for one hour. After

heat treatment, the samples were evaluated in low temperature seawater (30°C) with cyclic polarization, to determine the impact of the heat treatment on passive film stability and corrosion resistance. The temperatures used for the heat treatment were: 150, 300, 800 and 1000°C. Corrosion resistance was maintained below the crystallization temperature, and lost after prolonged aging at higher temperatures.

Potentiostatic Polarization. Potential step tests have been used to determine the potential at which the passive film breaks down on the reference material, Alloy C-22, and on the two amorphous metals of primary interest, SAM1651. During prolonged periods of at a constant applied potential, which are typically 24 hours in duration, the current is monitored as a function of time. In cases where passivity is lost, the current increases, and the test sample is aggressively attacked. In cases where passivity is maintained, the current decays to a relatively constant asymptotic level, consistent with the known passive current density. In these tests, periods of polarization are preceded by one hour at the open circuit corrosion potential. To eliminate the need for surface roughness corrections in the conversion of measured current and electrode area to current density, the SAM1651 coatings were polished to a 600-grit finish prior to testing. The constant potential denoted in the figures was applied after 1 hour at the open circuit corrosion potential (OCP).

Linear Polarization. The linear polarization method has been used as a method for determining the corrosion rates of the various amorphous metal coatings. The procedure used for linear polarization testing consists of the following steps: (1) hold the sample for ten (10) seconds at the open circuit potential (OCP); (2) beginning at a potential 20 mV below the OCP (OCP-20 mV), increase the potential linearly at a constant rate of 0.1667 mV per second, to a potential 20 mV above the OCP (OCP+20 mV); (3) record the current being passed from the counter electrode to the working electrode by the potentiostat, as a function of potential relative to the standard/silver silver-chloride (Ag/AgCl) reference electrode; and (4) determine the parameters in the cathodic Tafel line by performing linear regression on the voltage-current data from 10 mV below the OCP (OCP – 10 mV) to 10 mV above the OCP (OCP + 10 mV). The slope of this line is the polarization resistance, *Rp* (ohms), and is defined in the published literature [22]. While no values for the Tafel parameter (*B*) of Fe-based amorphous metals have yet been developed, it is believed that a conservative value of approximately 25 mV is reasonable, based upon the range of published values for several Fe- and Ni-based alloys [22]. The corrosion current density is then defined in terms of B, R_p and A, the actual exposed area of the sample being tested. The corrosion (or penetration) rate of an alloy can be calculated from the corrosion current density with through application of Faraday's Law [23-24].

Salt Fog Testing. Salt fog tests were conducted according to the standard General Motors (GM) salt fog test, identified as GM9540P. The four reference samples included Type 316L stainless steel, nickel-based Alloy C-22 (N06022), Ti Grade 7, and the 50:50 nickel-chromium binary.

Results

Composition and Structure. The compositions of melt-spun ribbon samples were verified with Energy Dispersive Spectroscopy (EDS). Figure 1 shows X-ray diffraction data for melt-spun ribbon (MSR) samples of iron-based amorphous metals identified as: SAM40 ($Fe_{52.3}Mn_2Cr_{19}Mo_{2.5}W_{1.7}B_{16}C_4$); SAM1651 ($Fe_{48}Cr_{15}Mo_{14}B_6C_{15}Y_2$); and SAM1651 + 3 atomic percent tungsten, which is designated SAM8 ($Fe_{46.6}Cr_{14.6}Mo_{13.6}W_3B_{5.8}C_{14.6}Y_{1.9}$). All were found to be completely amorphous.

Thermal Stability. SAM1651 has a glass transition temperature of ~584°C, a crystallization temperature of ~653°C, a melting point of ~1121°C, and a reduced glass transition temperature of ~0.55. The critical cooling rate of SAM1651 has been determined to be ≤ 80 K per second. The yttrium addition to this material was found to lower the critical cooling rate, and to enhance glass-forming ability.

Hardness. Such materials are extremely hard, and provide enhanced resistance to abrasion and gouges (stress risers) from backfill operations, and possibly even tunnel boring. The hardness of HVOF SAM1651 ranges from 857 to 997 VHN (kg mm^{-2}) with a 300-gram load, and 907 to 1154 VHN with a 100-gram load.

Repassivation Potential. CP data for a wrought prism of nickel-based Alloy C-22, a drop-cast ingot of iron-based SAM1651 amorphous metal, and a melt-spun ribbon of SAM8 (SAM1651 or SAM7 + 3 atomic percent tungsten), all obtained with 5M $CaCl_2$ at 105°C is shown in Figure 2. During this test, both SAM1651 and SAM8 showed passive film stability comparable to (or better than) that of wrought Alloy C-22. The addition of 3 atomic-percent tungsten to the SAM1651 enhanced the passive film stability, and also yielded more ductile and damage-tolerant amorphous metal ribbons.

Breakdown Potential. Current transients were measured at various levels of constant applied potential (100 to 800 mV vs. OCP) in seawater at 90°C, for a 600-grit polished SAM1651 HVOF coating on Type 316L stainless steel (serial number E316L409), and are shown in Figure 3. These measured transients are indicative of good passive-film stability, which is comparable to that of wrought Alloy C-22. To eliminate the need for surface roughness corrections in the conversion of measured current and electrode area to current density, the SAM1651 coating was polished to a 600-grit finish prior to testing. Passive film breakdown on the HVOF coating of SM1651 occurred at an applied potential between 500 and 600 mV vs. OCP, with a clear loss of passivity at 700 mV. The coating represented by this figure is one of the first known thermal spray coatings with the SAM1651 composition.

Current transients were measured at various levels of constant applied potential (100 to 450 mV vs. OCP) in 5M $CaCl_2$ at 105°C, for a polished SAM1651 HVOF coating on a Type 316L stainless steel (serial number E316L475), and are shown in Figure 4. Passive film breakdown on the HVOF coating of SAM1651 occurred at an applied potential between 360 and 400 mV vs. OCP, with a clear loss of passivity at 450 mV.

Potential-step testing in deaerated seawater heated to 90°C has been performed with SAM1651 and Alloy C-22 thermal spray coatings, as well as wrought Alloy C-22, as

shown in Figure 5. In this series of experiments, passive film breakdown on wrought Alloy C-22 occurred at a potential of approximately 600 mV above the open circuit corrosion potential. Passive film breakdown on the SAM1651 HVOF coating occurred at an applied potential between 500 and 600 mV, whereas breakdown on the Alloy C-22 HVOF coating occurred at approximately 400 mV. In near-boiling seawater, the passive film stability of SAM1651 is comparable to that of wrought Alloy C-22, and superior to that of Alloy C-22 HVOF coatings.

Potential-step testing has been performed on HVOF coatings of SAM1651 on Type 316L stainless steel (serial number E316L475) in extremely aggressive 5M $CaCl_2$ heated to 105°C, as shown in Figure 6. In this series of experiments, passive film breakdown on wrought Alloy C-22 occurred at a potential of 240 mV above the open circuit corrosion potential, with evidence of repassivation at potentials above 400 mV. Even with the possible repassivation at higher potential, the window of vulnerability between 240 to 400 mV is problematic for the reference material. Passive film breakdown on the SAM1651 HVOF coating occurred at a significantly higher applied potential, between 360 and 400 mV, whereas passive film breakdown on thermally sprayed Alloy C-22 was virtually spontaneous. It is therefore concluded that the SAM1651 coating may provide advantages for operation in hot concentrated chloride brines with aggressive divalent cations such as calcium.

Corrosion Rates. Linear polarization was used to determine the approximate corrosion rates of SAM1651 HVOF coatings and wrought nickel-based Alloy C-22 in three relevant environments, natural seawater at 30 and 90°C, and in 5M $CaCl_2$ at 105°C. Values of the corrosion potential and corrosion rate are summarized in Figures 7 and 9. In seawater at 30°C, the corrosion rates of HVOF SAM1651 coatings exhibited comparable to slightly higher corrosion rates than either wrought sample of Alloy C-22. As the temperature of the seawater was increased to 90°C, the corrosion rates of HVOF SAM1651 coatings exhibited comparable to slightly lower corrosion rates than either wrought sample of Alloy C-22. In general, corrosion rates trended to higher values with increasing temperature, as expected. In calcium chloride at 105°C, the corrosion rates of HVOF SAM1651 coatings were slightly lower than that of HVOF Alloy C-22; and slightly greater than those of wrought Alloy C-22. In general, the corrosion rates observed in the hot calcium chloride (105°C) were higher than those observed in the heated seawater (90°C).

Salt Fog Resistance. Salt fog testing was conducted on several thermal spray coatings, including HVOF coatings of Alloy C-22, Type 316L stainless steel, SAM40 (also referred to as DAR40), SAM1651 and other amorphous-metal formulations of interest. After 13 cycles in the GM9540P salt fog test, the HVOF coatings of Type 316L stainless steel and SAM40 showed substantial corrosion. Very slight rust spots were observed on the Alloy C-22 coating. In contrast, the SAM1651 formulation showed no corrosion at 30 cycles. The testing was continued to more than 54 cycles, with no evidence of corrosion observed with SAM1651 and other amorphous-metal formulations of interest.

Conclusions

SAM1651 has a low critical cooling rate (CCR), due to the addition of yttrium (Y), which enables it to be rendered as a completely amorphous thermal spray coating. The yttrium addition increases the viscosity of the alloy, thereby slowing the nucleation and growth kinetics of crystalline phases. Unfortunately, such increases in viscosity also make this material relatively difficult to gas atomize, with the powders having irregular shapes. Such non-spherical particle morphology causes pneumatic conveyance of the SAM1651 powder during thermal spray operations to be difficult. The production of nearly spherical gas-atomized SAM1651 powder with acceptable flow characteristics has required extensive process optimization.

The hypothesis that the corrosion resistance of Fe-based amorphous metals can be enhanced through application of heuristic principles related to the additions of chromium, molybdenum, tungsten and yttrium has been tested with SAM1651 and SAM8 formulations, and found to have merit. Electrochemical tests show that passive film stability comparable to that of nickel-based Alloy C-22 can be achieved with enhanced Fe-based amorphous metals in 5M $CaCl_2$ at 105°C and seawater at 90°C.

Thermal spray coatings produced with early Type 316L stainless steel, SAM35, SAM40, SAM40X3 exhibited rusting after 13 cycles in the standardized salt fog tests. However, dense and pore-free thermal spray coatings of SAM1651 showed no corrosion after more than 54 cycles in standard salt fog tests.

Acknowledgments

This work was done under the auspices of the U.S. DOE by UC, Lawrence Livermore National Laboratory (LLNL) under Contract No. W-7405-Eng-48. Work was sponsored by the United States Department of Energy (DOE), Office of Civilian and Radioactive Waste Management (OCRWM); and Defense Advanced Research Projects Agency (DARPA), Defense Science Office (DSO). The guidance of Leo Christodoulou at DARPA DSO and of Jeffrey Walker at DOE OCRWM is gratefully acknowledged.

References

1. D. Chidambaram, C. R. Clayton, M. R. Dorfman, Surface and Coatings Technology, **176**, 307-317 (2004).
2. D. E. Polk, B. C. Giessen, Overview of Principles and Applications, Chapter 1, Metallic Glasses, J. J. Gilman, H. J. Leamy, Eds., ASME, Metals Park, OH, pp. 2-35, 1978.
3. R. M. Latanison, Corrosion Resistance of Metastable Alloys Processed by Rapid Solidification, Workshop on Amorphous Metals and Semiconductors, EPRI, May 12-18, 1985.
4. K. Kishitake, H. Era, F. Otsubo, J. Thermal Spray Technology, **5** (2), 145 (1996).
5. S. Pang, T. Zhang, K. Asami, A. Inoue, Materials Transactions, **43** (8), 2137-2142 (2002).
6. S. J. Pang, T. Zhang, K. Asami, A. Inoue, Acta Materialia, **50**, 489-497 (2002).
7. H. Shinimiya, A. Nakazawa, Z. Kato, A. A. El Moneium, Y. Niizeki, K. Asami, K. Hashimoto, Paper 319, 208th ECS Meeting, Los Angeles, CA, October 16-21, 2005.
8. J. C. Farmer, J. J. Haslam, S. D. Day, T. Lian, R. Rebak, N. Yang, L. Aprigliano, PVP2006-ICPVT11-93835, Proc. ASME PVP Division Conf., July 23-27, 2006.
9. J. C. Farmer, J. J. Haslam, S. D. Day, D. J. Branagan, C. A. Blue, J. D. K. Rivard, L. F. Aprigliano, N. Yang, J. H. Perepezko, M. B. Beardsley, PVP2005-71664, Proc. ASME PVP Division Conf., Denver, Colorado, July 17-21, 2005.
10. J. C. Farmer et al., UCRL-TR-206717, LLNL, Livermore, CA, September 28, 2004.
11. F. Guo, S. J. Poon, G. J. Shiflet, Metallic Appl. Physics Letters, **83** (13), 2575-2577 (2003).
12. Z. P. Lu, C. T. Liu, W. D. Porter, Metallic Appl. Physics Letters, **83** (13), 2581-2583 (2003).
13. V. Ponnambalam, S. J. Poon, G. Shiflet, J. Mater. Res., **19** (5), 1320, 2004.
14. D. J. Branagan, U.S. Pat. Appl. 20040250929, December 16, 2004.
15. D. J. Branagan, Properties of Amorphous/Partially Crystalline Coatings, United States Patent Application No. 20040253381, Filed December 16, 2004.
16. C. K. Saw, in X-ray Scattering Techniques for Characterization Tools in the Life Sciences, Nanotechnologies for the Life Science, Challa Kumar, Ed., Wiley-VCH Verlag GmbH and Company, KGaA, Weinheim, 2006.
17. C. K. Saw and R. B. Schwarz, J. Less-Common Metals, **140**, 385-393 (1988).
18. Standard G 5-94, 1997 ASTM Standards, Section 3, Vol. 3.02, pp. 54–57, 1997.
19. Standard G 5-87, 1989 ASTM Standards, Section 3, Vol. 3.02, pp. 79–85, 1989.
20. J. R. Scully, J. L. Hudson, T. Lunt, G. Ilevbare, B. Kehler, Final Report, TRW/DOE YMP Purchase Order Number A10762JM8A, September 30, 1999.
21. K. A. Gruss, G. A. Cragnolino, D. S. Dunn, N. Sridar, Paper 149, Corrosion 98, NACE, Houston, TX, 1998.
22. R. S. Treseder, R. Baboian, C. G. Munger, in NACE Corrosion Engineer's Reference Book, 2nd Edition, NACE, Houston, TX, pp. 65-66, 1991.
23. D. A. Jones, in Principles and Prevention of Corrosion, 2nd Edition, Prentice Hall, Upper Saddle River, NJ, pp. 75–76, 1996.
24. A. J. Bard, L. R. Faulkner, Electrochemical Methods, Fundamentals and Applications, John Wiley and Sons, New York, NY, p. 67, 1980.

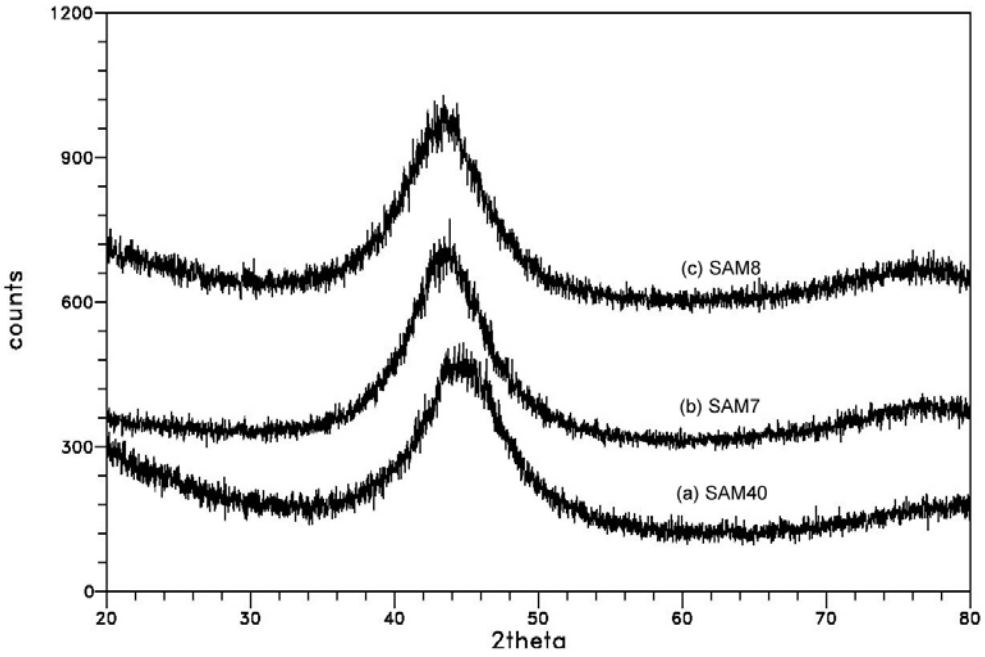

Figure 1 – This figure shows X-ray diffraction data for melt-spun ribbon (MSR) samples of iron-based amorphous metals identified as: SAM40; SAM7, which is similar to SAM1651 and SAM8.

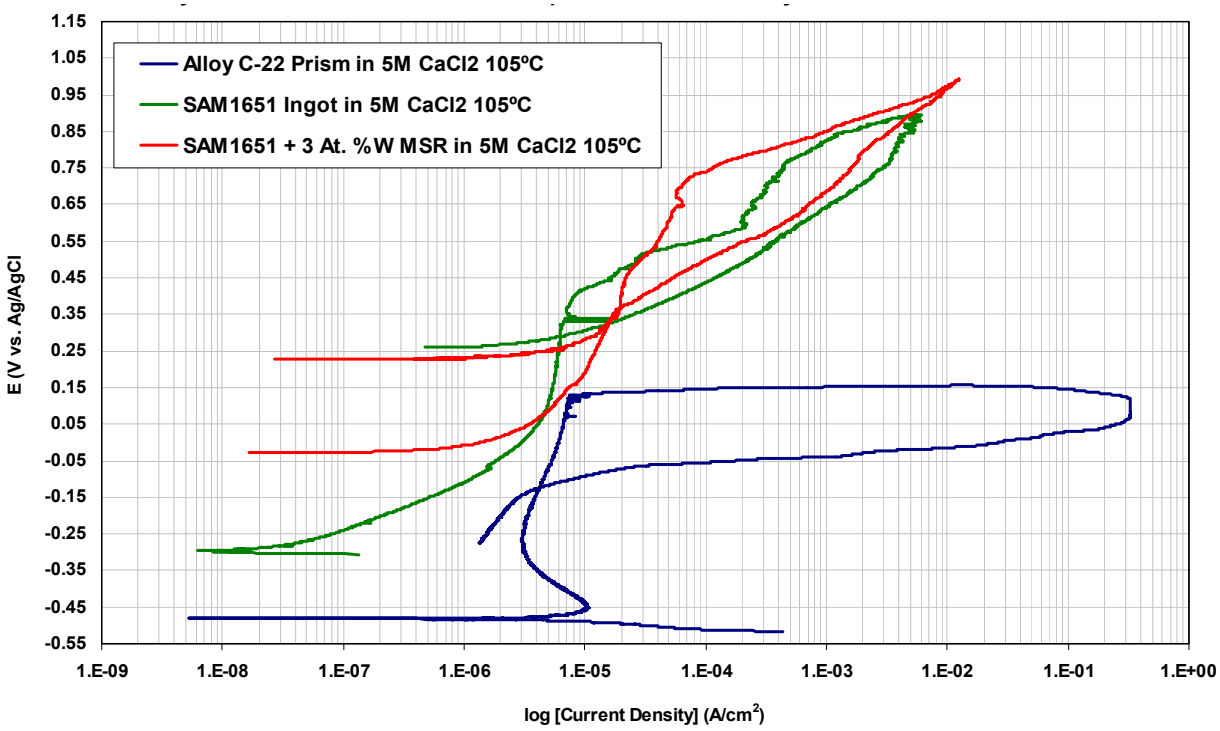

Figure 2 – Cyclic polarization testing with a 5M $CaCl_2$ test solution at 105°C. Data obtained with a melt-spun ribbon of SAM8 (SAM1651 + 3 atomic percent tungsten), a drop-cast ingot of iron-based SAM1651, and a wrought prism of nickel-based Alloy C-22 are compared.

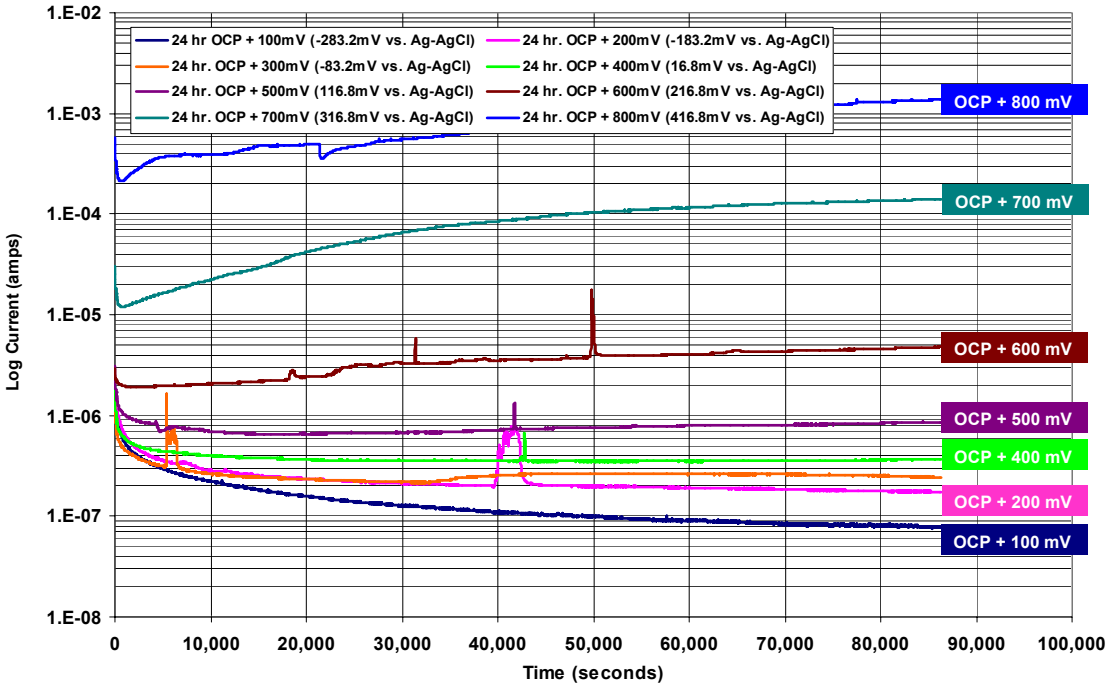

Figure 3 – Current transients were measured at various levels of constant applied potential (100 to 800 mV vs. OCP) in seawater at 90°C for a 600-grit polished SAM1651 HVOF coating on Type 316L stainless steel (serial number E316L409).

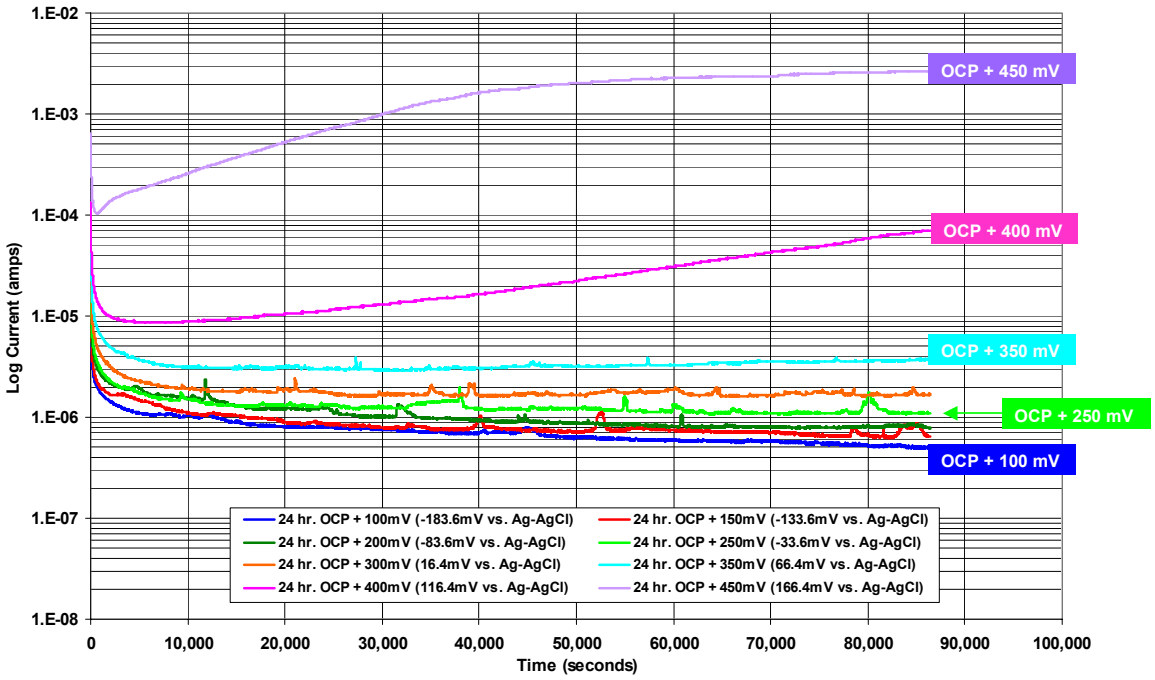

Figure 4 – Current transients wee measured at various levels of constant applied potential (100 to 450 mV vs. OCP) in 5M $CaCl_2$ at 105°C, for a polished SAM1651 HVOF coating on a Type 316L stainless steel (serial number E316L475).

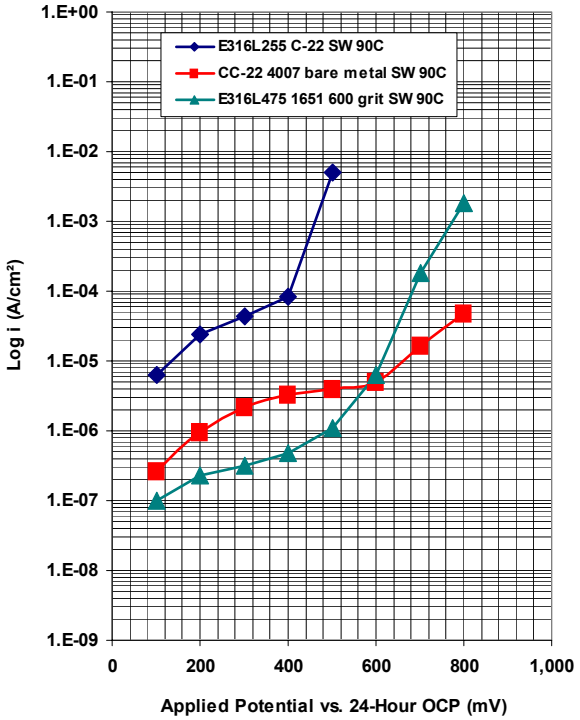

Figure 5 – Potential-step testing in deaerated seawater heated to 90°C has been performed with SAM1651 and Alloy C-22 thermal spray coatings, as well as wrought Alloy C-22.

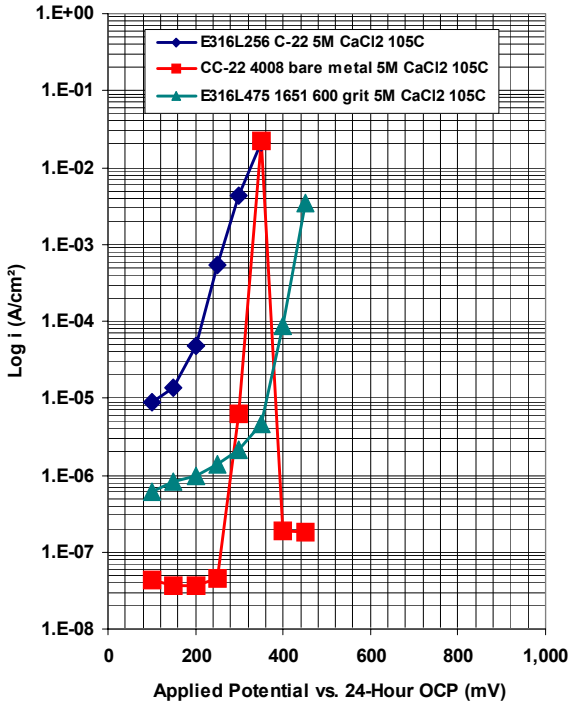

Figure 6 – Potential-step testing has been performed on HVOF coatings of SAM1651 on Type 316L stainless steel (SN # E316L475) in extremely aggressive 5M $CaCl_2$ heated to 105°C.

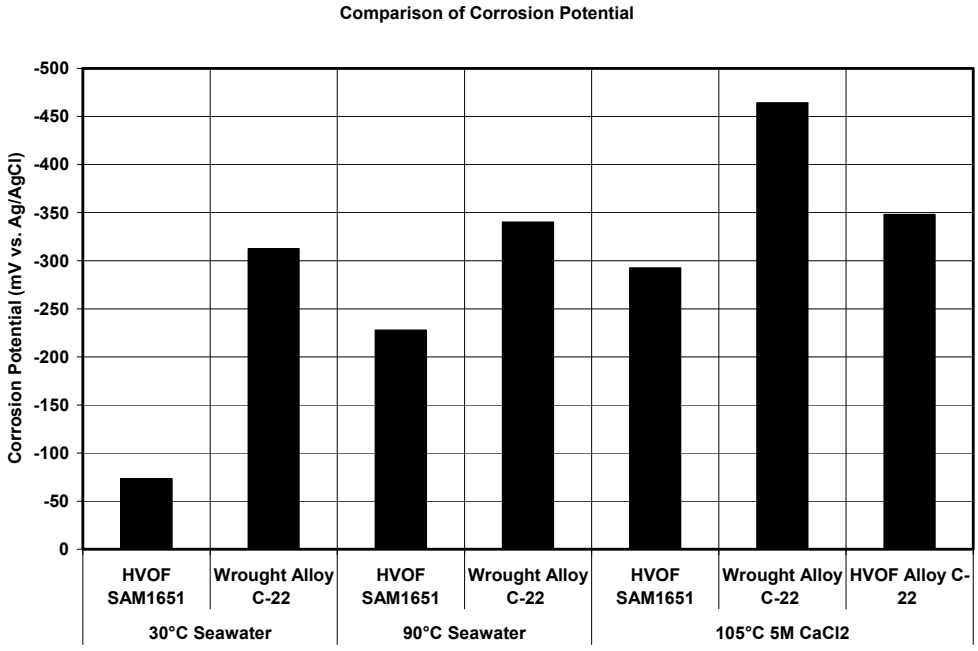

Figure 7 – The corrosion potentials for the thermal spray coatings of SAM1651 and the reference material (wrought nickel-based Alloy C-22) in three relevant environments, Half Moon Bay seawater at two temperature levels, and in hot concentrated calcium chloride (5M $CaCl_2$ at 105°C) are summarized.

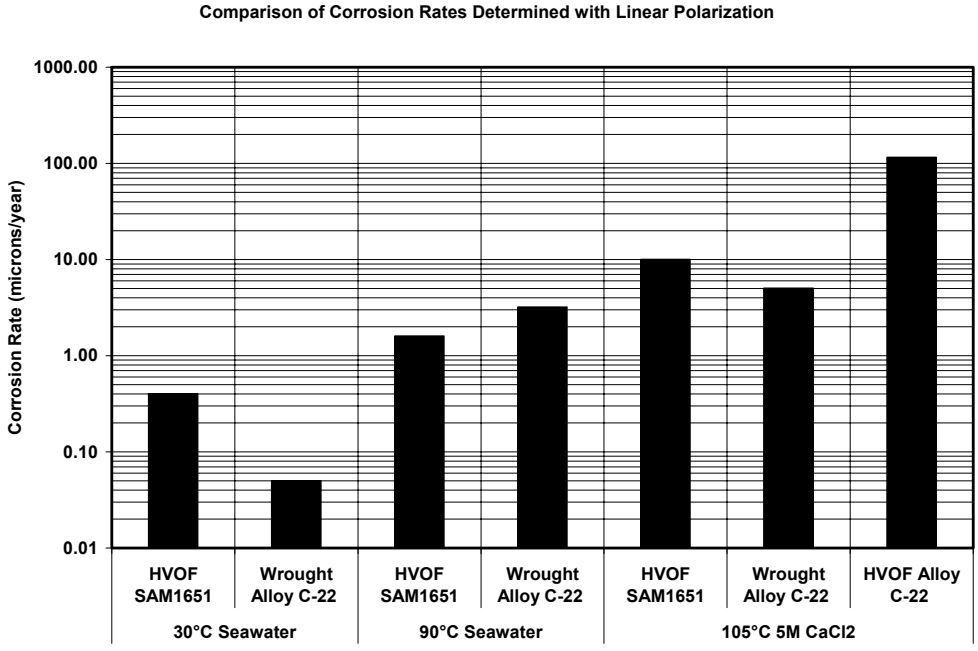

Figure 8 – Values of the polarization resistance were converted to corrosion rates for the thermal spray coatings of SAM1651 and wrought nickel-based Alloy C-22 in three relevant environments, natural seawater at 30 and 90°C, and in 5M $CaCl_2$ at 105°C.